CHAPTER V

PREPARATION OF CELLULOSE SHEETS CONTAINING SILVER/MAGNETIC PARTICLES FOR MAGNETICALLY AND ELECTRICALLY RESPONSIVE MATERIAL APPLICATION

5.1 Abstract

In the present study, the magnetically and electrically responsive bacterial cellulose (BC) was successfully prepared by step-wised synthesis of magnetic particles (Fe_3O_4) and silver particles (Ag) into BC matrix. The magnetic and silver particles were step-wised synthesized into BC matrix by using the ammonia gas-enhancing *in situ* co-precipitation method and the sodium borohydride-enhancing *in situ* synthesis method, respectively. Firstly, BC pellicle was immersed in an aqueous solution containing $FeCl_3$ and $FeSO_4$. After the iron ions absorbed-BC was treated with ammonia gas, the absorbed Fe^{2+} and Fe^{3+} ions were precipitated to be Fe_3O_4 particles inside BC. Then the Ag particles were synthesized into the magnetic particle-incorporated BC pellicle by immersing the as-prepared sample in aqueous $AgNO_3$ solution. The Ag^+-saturated sample was then immersed in the sodium borohydride ($NaBH_4$) solution. After immersing in the $NaBH_4$ solution, the absorbed-Ag^+ ions were reduced by $NaBH_4$ to form silver particles inside the magnetic particle-incorporated BC. The obtained bacterial cellulose pellicles were rinsed with a large amount of distilled water until it was neutral. Finally, the magnetic and silver particle incorporated- bacterial cellulose were freeze dried and kept in a desicator. The formation of magnetic and silver particles inside bacterial cellulose matrix was investigated by scanning electron microscopy (SEM), X-ray diffraction (XRD), and energy dispersive X-ray (EDX). The percentage loading of each particle in bacterial cellulose matrix were determined by thermogravimetric analysis (TGA). Finally, the magnetic field responsive and electric field responsive behaviors of the as-prepared samples were studied by vibrating sample magnetometry (VSM) and two point probe conductivity meter, respectively.

5.2 Introduction

The magneto-active materials and electro-active materials are specific subsets of smart materials in which their physical properties can adaptively change relatively to the changing of an external magnetic field (Filipcsei, Csetneki, Szilágyi, & Zrínyi, 2007) or external electric field (Paquette, Kim, & Kim, 2005), respectively. Now a day, these magnetic and electric field stimuli responsive materials have attracted more attention to the researchers because of its wide variety of applications such as actuator (Hiamtup, Sirivat, & Jamieson, 2008), sensor (Thuwachaowsoan, Chotpattananont, Sirivat, Rujiravanit, & Schwank, 2007; Epstein & Miller, 1996), information storage (Dikeakos et al., 2003), electromagnetic interference shielding paper (Fugetsua, Sanob, Sunadac, Sambongic, Shibuyac, Wangd, & Hirakid, 2008) and magnetically and electrically stimuli control released hydrogel (Tartaj, Morales, Veintemillas-Verdaguer, Gonzalez-Carreno, & Serna, 2003; Niamlang, & Sirivat, 2009). Generally, the magneto-active materials such as magnetorheological (MR) elastomers are elastomeric materials containing magnetizable components (Davis, 1999). The embedded magnetic particles give potential magnetizability to the otherwise magnetically inert elastomers (Davis 1999). Whereas, the electro-active materials such as Ionic polymer–metal composites (IPMCs) are electro-active polymers in which conductive particles are dispersed in a polymer matrix that be able to actuate under a low driving voltage input (Paquette, Kim, & Kim, 2005). Therefore, these magneto-active materials and electro-active materials were composed of two major components; magneto- or electro-active fillers and supporting matrix.

Among the several kinds of magneto-active fillers, magnetic nanoparticles were received more attention due to their unique magnetic properties. Magnetic nanoparticles are nanoparticles of iron oxides. In nature, iron oxides exist in various forms including hematite (α-Fe_2O_3), maghemite (γ-Fe_2O_3) and magnetite (Fe_3O_4) (Cornell & Schwertmann, 2003). Among the three forms of iron oxides, magnetite (Fe_3O_4) is exhibited the strongest magnetism of any transition metal oxides (Cornell & Schwertmann, 2003; Majewski & Thierry, 2007). Another important property of the magneto-active fillers is the superparamagnetic property. This property was

directly depended on their particle size of the magnetic particles. Lower than approximately 100 nm in diameter, the magnetic particle were exhibited the superparamagnetic property which no longer exhibits a history-dependent behavior or hysteresis (Wang *et al.*, 2004). The superparamagnetic materials are different from permanent magnet in that the magnetic interactions of nanoparticles of iron oxide are induced by external magnetic field while without external magnetic field, nanoparticles of iron oxide no longer show magnetic interaction (Neuberger, Schopf, Hofmann, Hofmann, & Rechenberg, 2005). Accordingly, there are two main requirements for being as the magneto-active fillers which are the as-synthesized iron oxide particles should be in the form of magnetite and the diameter of the as-synthesized iron oxide particles should be lower than 100 nm (Wang *et al.*, 2004).

Almost of the electro-active fillers are conductive materials such as gold particles, palladium particles, silver particles, nickel particles, copper particles, conductive polymer, graphite and carbon fiber. Among these several kinds of conductive material, silver is one of the most interesting materials due to its excellent electrical, thermal, optical and/or catalytic properties (Lu, & Chou, 2008). Silver bulk exhibited the high electrical conductivity with 10^6 S/cm. Recently, nanometer-scaled silver have received a great deal of attention in various potential applications, such as conductors, catalysts, chemical sensors, etc. (Haes, & Van Duyne, 2003; Magdassi et al., 2003; Nie, & Emory, 1997; Pradhan, Pal, & Pal, 2002; Ye, Lai, Liu, & Tholen, 1999). Due to their small sizes and large surface-to-volume ratios, nanometer-scaled silver have superior properties compared to their bulk counterparts, they are promising candidates for novel nanoscale electronic, optical and mechanical devices. In order to achieve the high efficiency of electrical conduction, the most importance requirement is the connection of as-prepared nanometer-scaled silver; the particles need to be well connected to form the conduction pathway (Zhang, Moon, Lin, Agar, & Wong, 2011). Anyways, silver is a high value element. High percent incorporation of silver was resulted in high overall cost of the product. In order to get the effective conductivity with optimizing of the product cost, the lowest amount with well connected of silver particles are the most important requirement (Bao, Wei, & Xiao, 2007).

Bacterial cellulose (BC) is high purified nanofibrous cellulose produced from the metabolism process of *Acetobacter xylinum* (*A. xylinum*) bacteria by using glucose as a carbon source. BC is produced in the form of multilayer structure of three-dimensional nonwoven network of nanofibrous cellulose. Basically, BC has the same chemical structure as vascular plant cellulose, linear α–1,4–glucan chains (Czaja, Romanovicz, & Malcolm Brown, 2004) but the physical structure of the BC is totally different from the vascular plant cellulose. The three-dimensional structure was found only in the BC but not in the vascular plant cellulose (Rezaee, Solimani, & Forozandemogadam, 2005; Wan, Hong, Jia, Huang, Zhu, Wang, & Jiang, 2006; Grzegorczyn & Ezak, 2007). This structure of BC resulted in high cellulose crystallinity (60–80%) and as high Young's modulus of 138 GPa and tensile strength of at least 2 GPa, which are almost equal to those of aramid fibers (Li, Chen, Hu, Shi, Shen, Zhang, & Wang, 2009). The nanometer scale diameter of BC fiber, about 100 times smaller than fibrils in plant cellulose, leads to a large surface area that can hold large amount of water (up to 200 times of its dry mass) and display a great elasticity and a high wet strength. (Klemm, Schumann, Udhardt, & Marsch, 2001; Czaja, Young, Kawecki & Brown, 2007). One of the most important features of BC is its chemical purity. BC is free of lignin and hemicelluloses, whereas plant cellulose usually associates with these chemicals. Furthermore, the high chemical purity and high liquid absorption capacity resulted in a good biocompatibility of BC. These unique physical properties, mechanical properties, and chemical purity of BC leading to wide range of applications such as paper industrial, headphone membranes, food industrial (Li, Chen, Hu, Shi, Shen, Zhang, & Wang, 2009), biomaterials including temporary skin substitute, artificial blood vessels (Czaja, Young, Kawecki, & Brown, 2007; Kamel, 2007) and membrane for pervaporation of water-ethanol binary mixtures (Dubey, Saxena, Singh, Ramana & Chauhan, 2002). Moreover, BC also serves as an applicable matrix for impregnating of nanoparticles or nanowires such as cadmium sulfide nanoparticles (Li, Chen, Hu, Shi, Shen, Zhang, & Wang, 2009), silver chloride nanoparticles (Hu, Chen, Li, Shi, Shen, Zhang, & Wang, 2009), silver nanoparticles (Maneerung, Tokura, & Rujiravanit, 2008) and titania nanowires (Zhang & Qi, 2005).

According to the unique properties of magnetic and silver nanoparticles, the magneto- and electro-active material could achieve by synthesizing of the magnetic and silver nanoparticles into the same supporting matrix. Therefore, the composite material, containing magnetic and silver nanoparticles was showed the properties of each containing particles in which the magnetic field responsive properties from magnetic nanoparticles and electric field responsive from silver nanoparticles. However, the supporting matrix has to provide the final structure of as-prepared product that could achieve the requirements of magnetic nanoparticles and silver nanoparticle. For the magnetic nanoparticle, there are two main requirements for being as the magneto-active fillers which are the as-synthesized iron oxide particles should be in the form of magnetite and the diameter of the as-synthesized iron oxide particles should be lower than 100 nm (Wang *et al.*, 2004). Whereas, the lowest amount with well connected of particles was the most important requirement of silver nanoparticle in order to function as the electro-active fillers (Bao, Wei, & Xiao, 2007).

In this study, the magneto- and electro-active material was prepared by incorporating of magnetic and silver particles into the nanofibrous matrix of BC. The magnetic and silver particles were step-wised synthesized into BC matrix by using the ammonia gas-enhancing *in situ* co-precipitation method and the sodium borohydride-enhancing *in situ* synthesis method, respectively. The magnetic nanoparticles were firstly incorporated into BC matrix. Then, the appropriate amounts of silver particle were synthesized into the magnetic particles-incorporated BC pellicle. Due to the nanofibrous structure of BC matrix, the as-prepared magnetic and silver particle-incorporated BC samples were expected to exhibit the properties of both magnetic and silver particle. According to these proposed process, the magneto- and electro-active material were successfully prepared by step-wised incorporating of magnetic and silver particle into the BC matrix, respectively.

5.3 Experimental

5.3.1 Materials

Acetobacter xylinum (strain TISTR 975), an isolated strain in Thailand, was supplied from the Microbiological Resources Centre, Thailand Institute of Scientific and Technological Research (TISTR). Analytical grade anhydrous of D-glucose was obtained from Ajax Finechem. Bacteriological grade of yeast extract powder was purchased from HiMedia. Analytical grade ferric chloride ($FeCl_3 \cdot 6H_2O$) and ferrous sulphate ($FeSO_4 \cdot 7H_2O$) were purchased from Riedel-deHaën and Ajax Finechem, respectively. Analytical grade silver nitrate and laboratory grade sodium borohydride were obtained from Fisher Scientific and CARLO ERBA, respectively. Other chemical reagents used in this study were analytical grade and used without further purification.

5.3.2 Production of bacterial cellulose

The production process for BC was similar to our previous work (Katepetch, & Rujiravanit, 2011). Briefly, the pre-inocula for all the experiments were prepared by transferring a single colony of *A. xylinum* bacteria (strain TISTR 975) into 20 ml of a liquid culture medium, which was composed of 4 wt% g of D-glucose anhydrous, 1 wt% of yeast extract powder. After 24 h of cultivation at 30°C, 2.5 ml of the cell suspension was introduced into a 200 ml-Erlenmeyer flask containing 25 ml of fresh liquid culture medium and then cultivated at 30°C for 4 days. The obtained BC was purified by boiling in 1 % NaOH for 2 h. The boiling step was repeated twice. The purified BC was then treated with 1.5 % acetic acid for 30 min, and finally washed in a tap water until BC pellicles became neutral. The porous structure of BC was preserved by immersing into the distilled water and kept into a refrigerator at 4°C prior to use.

5.3.3 Ammonia gas-enhancing in situ co-precipitation of magnetic particles into BC pellicles

Magnetic particle incorporated-BC pellicles were prepared by immersing the BC pellicles (ca.99.5% water content) in an aqueous iron salt solution

at 60°C. The aqueous iron salt solution contained $FeCl_3$ and $FeSO_4$ with the mole ratio of the Fe^{3+} to Fe^{2+} ions to be fixed at 2:1. The total concentration of aqueous iron ion was varied to be 0.01 M, 0.05 M, 0.1 M, 0.5 M and 1 M, respectively. After immersion of the BC pellicles into the iron salt solution for 1 h, the excess iron, yellowish-brown particles, on the surface of the BC pellicles was rinsed with distilled water. After washing, the iron ion-absorbed BC pellicles were kept inside 500 ml wide-neck round bottom flask (a reaction vessel) and pre-treated with nitrogen gas for 10 min in order to eliminate oxygen gas before further treating with ammonia gas. The volumetric flow rate of ammonia gas was controlled by a flow meter. The experimental set up for the ammonia gas-enhancing *in situ* synthesis method was showed in the figure 5.1. When ammonia gas was purged into the reaction vessel, the color of iron ion-saturated BC pellicles was gradually changed. After 30 min of ammonia gas treatment, the as-prepared magnetic particle incorporated-BC pellicles had dark brown color. The obtained BC pellicles were rinsed with a large amount of distilled water until neutral and then sonicated for 20 min in order to remove any loosely bound particles. Finally, the as-prepared magnetic particle-incorporated BC pellicles were immersed in the distilled water prior to use.

5.3.4 *Sodium borohydride-enhancing in situ synthesis of silver particles into magnetic particle incorporated-BC pellicles.*

Silver particles were incorporated into the magnetic particle incorporated-BC pellicle by immersing the magnetic particle incorporated-BC pellicles in 0.01 M of the aqueous $AgNO_3$. The concentration of $AgNO_3$ solution was varied to be 0.01 M, 0.05 M, 0.10 M, respectively. After immersion of the magnetic particle incorporated-BC pellicle into the $AgNO_3$ solution for 1 h, the excess silver ions on the surface of the BC pellicles was rinsed with distilled water. After washing, the silver ion-absorbed BC pellicle was then immersed in 0.1 M Sodium borohydride ($NaBH_4$) solution. The concentrations of $NaBH_4$ were relatively fixed with the concentration of $AgNO_3$. The mole ratio of $NaBH_4$:$AgNO_3$ was fixed at 1:10 therefore the 0.01 M, 0.05 M and 0.10 M of $AgNO_3$ were corresponded to the 0.10 M, 0.50 M and 1.00 M of $NaBH_4$, respectively. After immersing in $NaBH_4$ for 30 min, the obtained BC pellicles were rinsed with a large amount of distilled water

until neutral and then sonicated for 20 min in order to remove any loosely bound particles. Finally, the obtained samples were freeze dried and kept in a desicator.

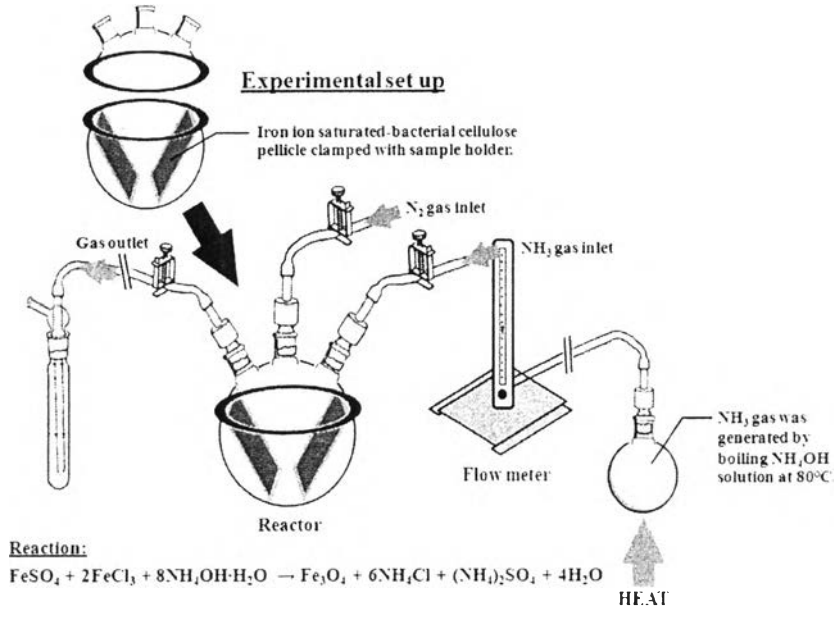

Figure 5.1 Schematic diagram of the laboratory set up for preparation of the magnetic particle-incorporated bacterial cellulose pellicle by ammonia gas-enhanced *in situ* co-precipitation method.

5.3.5 Characterization

The microstructure of the neat BC and magnetic and silver particle incorporated- BC was investigated by using the JEOL JSM-5200 scanning electron microscope (SEM). The crystal structure of Magnetic and Ag particle inside the as-prepared magnetic and silver particle incorporated-BC sample was studied by the X-ray diffraction (XRD) (Rigaku). The samples were scanned from 2□ = 10° to 2 □ = 70° at a scanning rate of 5° 2□/min. The thermal stability of the as-prepared magnetic and silver particle incorporated-BC sample and percent incorporation of magnetic and Ag particle inside the as-prepared magnetic and silver particle incorporated-BC sample were studied by using the thermogravimetric analysis (TGA, Perkin Elmer TGA7). The thermograms of the as-prepared ZnO particle

incorporated-BC sample was in the temperature range from 50 to 750 °C with heating rate of 10 °C/min in a flow of air at 20 ml/min.

5.3.6. *Vibrating sample magnetometry (VSM)*

The responsiveness to the magnetic field of the as-prepared magnetic particle-incorporated BC sample, as-prepared silver particle-incorporated BC sample and as-prepared magnetic and silver particle-incorporated BC sample were detected by vibrating sample magnetometer. Sample was inserted into a sample holder and vibrated within a magnetic field of up to 10,000 G. The magnetic moments of the as-prepared sample were recorded as a function of applied field at the temperatures of 300 K and the results were reported in term of a magnetic hysteresis loop (Jiles, 1991).

5.3.7 *The electrical conductivity*

The electrical conductivity of the as-prepared magnetic particle-incorporated BC sample, as-prepared silver particle-incorporated BC sample and as-prepared magnetic and silver particle-incorporated BC sample were measured following the method of Ludeelerd, Niamlang, Kunaruksapong, & Sirivat (2010). All as-prepared samples were cut into a dish shape with 1 cm in diameter. The Keithley, Model 8009 probe was used for measuring electrical conductivity of the as-prepared sample. The constant voltage was supplied by Keithley, Model 6517A which connecting to the measured-probes and the measured-probes were in contact with a surface of the as-prepared sample. The output current while applying voltage was measured. The output current was only measured in the linear Ohmic regime of each sample. The applied voltage and the resultant current were converted to the electrical conductivity the as-prepared sample by following equation

$$\sigma = 1/\rho = 1/(R_s \times t) = I/(K \times V \times t)$$

where σ is the specific conductivity (S/cm), ρ the specific resistivity (Ω cm), R_s the resistivity of the as-prepared sample (Ω), I the resultant current (A), K the geometric correction factor, V the applied voltage (voltage drop, V), and t the thickness of the as-prepared sample (cm).

5.4 Results and Discussion

5.4.1 The preparation of magnetic particle incorporated-BC by using the ammonia gas-enhancing in situ synthesis method

BC is purified cellulose which produced from *A. Xylinum* bacteria by using glucose as a carbon source. BC is firstly generated at the interface between air and the culture surface. Then, BC pellicle was generated a layer by layer slides steadily downwards as it thickens (Iguchi, Yamanaka, & Budhiono, 2000). BC fibrils is extruded passing through the cell membrane of *A. Xylinum* bacteria therefore diameter of BC fibrils were in the same range of nanometer scale diameter. *A. Xylinum* bacteria produce BC in order to protecting itself from environmental damaging so BC is produced in the form of nonwoven network structure. The surface and cross-sectional morphology of the neat BC is showed in the figure 5.2. According to the BC production process, the surface morphology of neat BC show the three dimensional non-woven network structure of nanofibrous cellulose with a fiber diameter of 55.00 ±10.54 nm (figure 5.2a). The cross sectional morphology of BC shows the multilayer structure of BC membranes that linked together with the nanofibrils cellulose (figure 5.2b). These unique nanometer scale structure of BC are provided a large amount of surface hydroxyl groups. Therefore, the BC fibrous exhibited the super hydrophilic surface with represented in the form of hydrogel or never-dried state of BC pellicle. This never-dried state of BC provided a good tunnel for iron ions penetration through inside BC which corresponded to the concept of *in situ* synthesis. Therefore, these unique physical structure of BC was firmly supported the ammonia gas-enhancing *in situ* synthesis method. The experimental set up for the ammonia gas-enhancing *in situ* synthesis method was showed in the figure 5.1. The BC pellicle was firstly immersed in the iron ions solution which containing of $FeCl_3$ and $FeSO_4$. During the immersion process BC pellicle in the iron ions solution, the iron ions, Fe^{3+} and Fe^{2+} were readily to penetrate though inside the BC matrix by passing through the microporous structure of BC pellicle. Moreover, the penetrated the iron ions, Fe^{3+} and Fe^{2+} were trapped inside BC by the electrostatic interaction between the polar groups at the surface of BC nanofibrils such as hydroxyl or ether groups. Then, the iron ion absorbed-BC pellicles were treated with ammonia gas.

While treating with ammonia gas, the absorbed Fe^{2+} and Fe^{3+} ions were precipitated to be magnetite particles inside the BC pellicles. The use of ammonia gas could achieve the homogeneous dispersion of the magnetic particles across the cross-sectional area of the as-synthesized BC pellicles since the ammonia gas is easier to penetrate through the BC pellicles than using concentrated liquid basic solutions. Moreover, ammonia gas could slightly increase pH of the sample and prevent the predominant precipitation of magnetic particles at the surface of bacterial cellulose pellicles (Katepetch, & Rujiravanit, 2011). By using the ammonia gas-enhancing *in situ* co-precipitation method, the oxygen gas could be eliminating by using N_2 gas flooding. The absent of oxygen gas could eliminate the impurities of other iron oxide which generated by side reaction with oxygen (Katepetch, & Rujiravanit, 2011). Hence, the homogeneously distribution of Fe_3O_4 particles in the matrix of BC were successfully achieved by using the ammonia gas-enhancing *in situ* co-precipitation method.

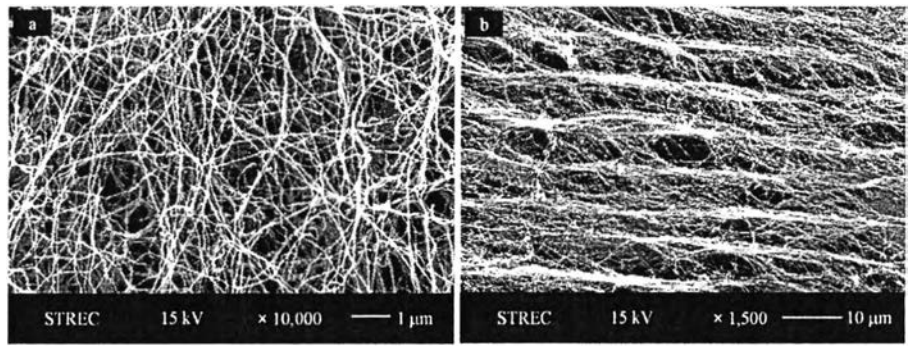

Figure 5.2 Surface and cross-sectional morphology of neat BC at the magnification of 10,000× (a) and 1,500× (b), respectively.

5.4.2 Morphology of the magnetic particle incorporated-BC prepared by ammonia gas-enhancing in situ synthesis method

The morphology of the as-prepared magnetic particle incorporated-BC samples were investigated by SEM. The figure 5.3 show the surface morphology of the as-prepared magnetic particle incorporated-BC samples, prepared by using ammonia gas enhanced *in situ* co-precipitation method by using 0.01 M (figure 5.3a),

0.05 M (figure 5.3b), 0.10 M (figure 5.3c), 0.50 M (figure 5.3d) and 1.00 M (figure 5.3e) of aqueous iron ion solution, respectively. Surface morphology of the as-prepared magnetic particle incorporated-BC sample were exhibited the three-dimensional non woven network structure of nanofibrous cellulose which composed of the incorporated- magnetic particle. Whereas, the unique multilayer structure of BC membranes was still observed in the cross-sectional morphology of BC (data were not show). At the 0.01 M and 0.05 M of iron ion concentration, the discrete particles of the incorporated-magnetic particles were observed at the surface of BC fibril. When concentration of the aqueous iron ion solution was increased from 0.05 M to 0.10 M and to 0.50 M, the incorporated-magnetic particles tended to aggregate and coat on the surface of BC fiber. At the 0.50 M of iron ion concentration, the incorporated-magnetic particles were completely coated on the surface of BC. Anyway, the incorporated-magnetic particles still increased with increasing of the concentration of iron ion from 0.50 M to 1.00M as evidenced by the increasing of the thickness of the coating layer (figure 5.3e). According to the advantages of the ammonia gas-enhancing *in situ* co-precipitation method, there was no change in the unique three-dimensional network structure of BC after incorporation of magnetic particles. The unique morphology of the as-prepared magnetic particle-incorporated BC sample was corresponded to the sodium borohydride-enhancing *in situ* synthesis in that the silver ions were firstly homogeneous incorporated into the porous structure of the as-prepared magnetic particle-incorporated BC sample. Then, the incorporated-silver ions were reduced to silver particles by using sodium borohydride as a reducing agent. The obtained magnetic and silver particle incorporated-BC sample were expected to be exhibited the homogeneous distribution of both magnetic and silver particles.

5.4.3 Thermogravimetric analysis of magnetic particle-incorporated BC prepared by ammonia gas-enhancing in situ synthesis method

The percent incorporation of magnetic particles in the as-prepared magnetic particle incorporated-bacterial cellulose samples were examined by using thermogravimetric analysis (TGA). In order to prevent the oxidation reaction between the as-prepared samples and oxygen in air, all thermograms were recorded

under nitrogen atmosphere. The investigating temperature was ranged from 50 °C to 750 °C. Figure 5.4 showed the TGA thermograms of neat BC and the as-prepared magnetic particle incorporated-BC samples prepared by ammonia gas-enhancing *in situ* co-precipitation method using 1 M, 0.5 M, 0.1 M, 0.05 M and 0.01 M aqueous iron ion solutions. The thermograms of neat BC showed the main weight loss between 275 °C to 375 °C as the result of the thermal decomposition of BC. These include depolymerization, further dehydration, degradation of the glucopyranosyl units and subsequent oxidation leaving behind charred residues (Roman & Winter, 2004). All thermograms of the as-prepared magnetic particle incorporated-BC appeared to be quite similar to the thermogram of neat BC in term of the degradation temperature by the occurrence of main weight loss between 275 °C to 375 °C. The percent incorporation of magnetic particles in the as-prepared magnetic particle incorporated-BC samples were determined by using TGA (Ghule *et al.*, 2006). The total percent weight loss of neat BC was 92.62 ±0.33 wt% and the residue from thermal decomposition of BC was 7.31 ±0.33%. The residue from thermal decomposition of BC was attributed to vestigial carbon of BC whereas the total percent weight loss of the as-prepared magnetic particle-incorporated BC sample prepared by ammonia gas-enhanced *in situ* co-precipitation method using 0.01 M, 0.05 M, 0.1 M, 0.50 M and 0.10 M aqueous iron ion solution were 72.32 ±0.24 wt%, 52.34 ±1.35 wt%, 41.00 ±1.48 wt%, 30.39 ±0.35 wt% and 17.36 ±0.11 wt%, respectively. The difference in percent weight loss between neat BC and the as-prepared magnetic particle-incorporated BC sample was attributed to be the percent incorporation of magnetic particle in the as-prepared magnetic particle-incorporated BC sample that were calculated to be 20.37 ±0.10 wt%, 40.36 ±1.01 wt%, 51.69 ± 1.15 wt%, 62.31 ±0.68 wt% and 75.30 ± 0.43 wt% for the conditions with using aqueous iron ion solutions to be 0.01 M, 0.05 M, 0.10 M, 0.50 M and 1.00 M respectively (as shown in Figure 5.4b). The percent incorporation of magnetic particle in the as-prepared magnetic particle incorporated-BC sample remarkably increased with increasing of the total concentrations of aqueous iron ion solutions from 0.01 M to 0.05 M and to 0.1 M. However, when the concentrations of aqueous iron ion solutions were further increased from the 0.1 M to 0.5 M and to 1 M, the percent incorporation of magnetic particle in the as-prepared magnetic particle

incorporated-BC sample were slightly increased and tended to reach equilibrium at a concentration of aqueous iron ion solution higher than 1 M.

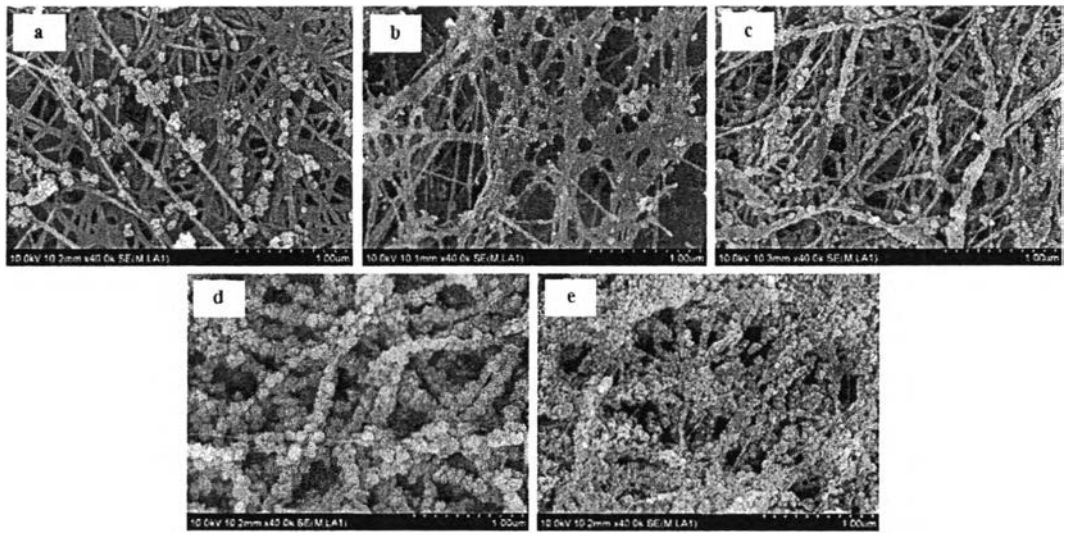

Figure 5.3 SEM images of magnetic particle-incorporated BC samples, prepared by ammonia gas-enhancing in situ co-precipitation method with 0.01 M (figure 5.3a), 0.05 M (figure 5.3b), 0.1 M (figure 5.3c), 0.5 M (figure 5.3d) and 1 M (figure 5.3e) of aqueous iron ion solution, at the magnification of 40,000×.

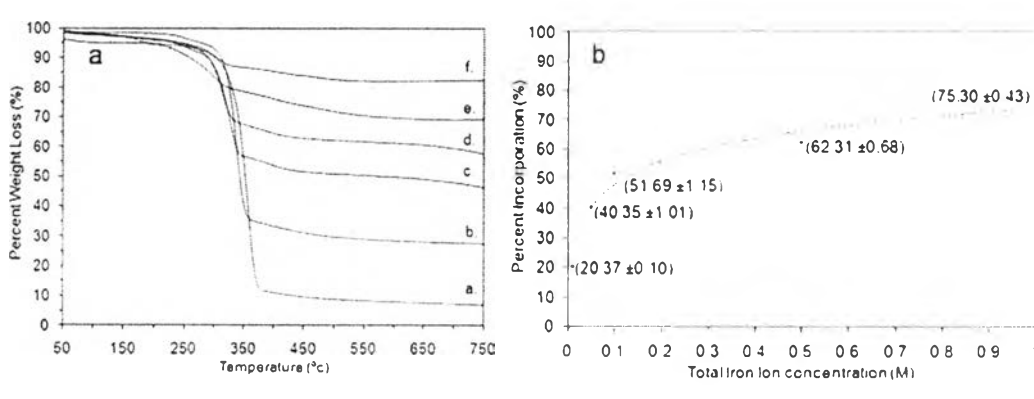

Figure 5.4 TGA thermograms of Neat BC (a) and magnetic particle incorporated-BC samples prepared by ammonia gas-enhancing *in situ* co-precipitation method using 0.01 M (b), 0.05 M (c), 0.10 M (d), 0.50 M (e) and 1.00 M (f) aqueous iron ion solutions. Inset showed the percent incorporation of magnetic particle in the magnetic particle incorporated-BC sample with increasing of the aqueous iron ion

concentration. The percent incorporation of magnetic particle is the difference in weight loss when compared to the neat BC.

5.4.4 *Magnetically responsive behavior of the as-prepared magnetic particle-incorporated BC samples*

The magnetically responsive behavior of the as-prepared magnetic particle-incorporated BC samples was determined by using vibrating sample magnetometry (VSM). The hysteresis loops of the as-prepared magnetic particle-incorporated BC samples at the temperatures of 300 K shown in figure 5.5a. Figure 5.5b show the magnified view of the corresponding loops at the temperatures of 300 K. The dependence of the magnetization (M) with the applied magnetic field (H) is described by the Langevin equation (Cornell & Schwertmann, 2003):

$M = M_S (\coth y - 1/y)$

where Ms is the saturation magnetization and $y = mH/k_BT$. (m is the average magnetic moment of an individual particle in the sample, k_B is the Boltzmann constant and T is temperature). At the temperature of 300 K, the saturation magnetizations of the as-prepared magnetic particle-incorporated BC samples prepared by ammonia gas-enhanced *in situ* co-precipitation method using 0.01 M, 0.05 M, 0.10 M, 0.50 M and 1.00 M aqueous iron ion solutions were 2.10 emu/g, 17.42 emu/g, 27.99 emu/g, 40.57 emu/g and 45.16 emu/g, respectively (Figure 5.5a). The increasing in saturated magnetization of the as-prepared magnetic particle incorporated-BC samples with increasing of the iron ion concentration were corresponded to the increasing in percent incorporation of magnetic particles in the as-prepared magnetic particle incorporated-BC sample. Therefore, the increasing in saturated magnetization of the as-prepared magnetic particle incorporated-BC sample was resulted from the increasing in percent incorporation of magnetic particles inside the as-prepared samples (Guo, Ye, Liu, Wu, Shen, & Shu, 2009).

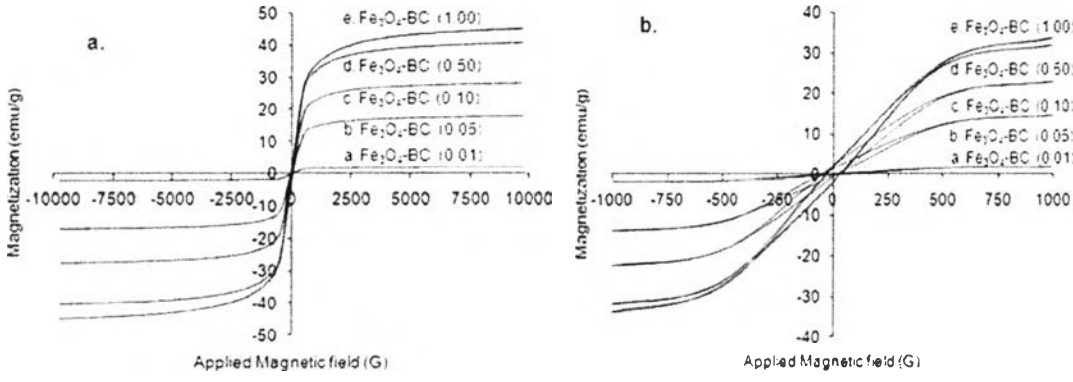

Figure 5.5 Magnetic hysteresis loop of magnetic particle incorporated-BC sample at the temperature of 300 K (a) and magnified view of its hysteresis loop (b).

The magnified view of the hysteresis loops of the as-prepared magnetic particle incorporated-BC sample at 300 K were shown in Figure 5.5b. When the concentration of aqueous iron ion solutions were increased from 0.01 M to 1.00 M, the larger hysteresis loops with the higher remnant magnetization (Mr) and the higher coercive field (Hc) were obtained. The remnant magnetizations were found to be 2.1 emu/g, 17.42 emu/g, 27.99 emu/g, 40.57 emu/g and 45.16 emu/g whereas the coercive fields were found to be 33.14 G, 34.30 G, 34.08 G, 34.16 G and 33.26 G for the samples prepared at the conditions of using 0.01 M, 0.05 M, 0.10 M, 0.50 and 1.00 M of aqueous iron ion solutions, respectively. The most important magnetic propertie for function as the magneto-active material was the superparamagnetic property. This property could determine by considering the magnified view of the magnetic hysteresis loop of the as-prepared magnetic particle incorporated-BC samples. The magnified view of the magnetic hysteresis loops with exhibited the coercive field lower than 100 G were classified to be a superparamagnetic material. According to the figures 5.5b, the as-prepared magnetic particle incorporated-BC samples were exhibited the coercive field of 33.14 G, 34.30 G, 34.08 G, 34.16 G and 33.26 G for the samples prepared at the conditions of using 0.01 M, 0.05 M, 0.10 M, 0.50 and 1.00 M of aqueous iron ion solutions, respectively. The obtained coercive fields of the as-prepared samples were much lower than the classifying limit (100 G)

therefore all of the as-prepared magnetic particle incorporated-BC samples were exhibited the superparamagnetic behavior.

5.4.5 *The preparation of magnetic and silver particle incorporated-BC by using the sodium bohohydride-enhancing in situ synthesis method*

In order to achieve the both magneto- and electro-active properties, the silver particles were synthesized into the as-prepared magnetic particle incorporated-BC sample. To obtain electrical conductivity, the silver volume fraction has to exceed the percolation threshold, where a percolated silver network is formed in the polymer matrix (Bao, Wei, & Xiao, 2007). For typical fillers, it is required very high fillers content in order to reach the percolation threshold for example: spherical particles were required the percent incorporation of fillers in the order of 16 to 30% by volume (Stauffer & Aharony, 1992). Higher aspect ratio of the filler helps to lower the percolation threshold. Consequently, silver flakes are usually used for these applications than spherical silver particles. Anyways, the percolation threshold of silver flakes remains quite high at close to 20 % by volume. Therefore, typically polymer based conductive formulations have very high silver loading (70-85 % by weight) (Bao, Wei, & Xiao, 2007). Because of the high cost of precious metals, such conductive formulations are usually very expensive. Hence, the lowest percent incorporation of the incorporated-particles with reaching to the percolation threshold is the most important requirement for achieving the effective conducting material. According to the literatures, the spherical particles were required the percent incorporation of fillers in the order of 16 to 30% by volume for achieving the percolation threshold (Stauffer & Aharony, 1992). The as-prepared magnetic particle incorporated-BC sample for being as the matrix in order to synthesize the silver particles were selected based on the remaining space for silver particles must be higher than 30%. The as-prepared magnetic particle incorporated-BC sample with 62.31 ±0.68 wt% of magnetic particles was selected for being as a matrix of silver particles.

The as-prepared magnetic particle incorporated-BC pellicles were firstly immersed in the silver nitrate solution. The remaining porous structure of the as-prepared magnetic particle incorporated-BC pellicles were resulted in the

homogeneous distribution of the absorbed-silver ions in the as-prepared BC pellicle. Then, the silver ions absorbed-magnetic particle incorporated-BC pellicles were immersed in the sodium borohydride solution. The absorbed-silver ions inside the as-prepared magnetic particle incorporated-BC pellicle were reduced to be the silver particle and coated on the magnetic particles coated-BC fibrils. By using this preparation method, the magnetic and silver particles were homogeneous incorporated into the BC matrix and the obtained silver and magnetic particle-incorporated BC samples were exhibited the effective magneto- and electro-active properties.

5.4.6 The crystal structure of Magnetic and Ag particle in the as-prepared magnetic and silver particle incorporated-BC sample

Crystal structures of the incorporated-magnetic and silver particles were examined by using XRD technique. The silver particle incorporated-BC samples as a control were prepared by immersing of BC pellicle in the 0.10 M of silver nitrate solution for 1 h. Then, the silver ion absorbed-BC pellicle was immersed in 1.00 M of sodium borohydride solution. After 30 min immersing in sodium borohydride solution, the as-prepared silver particle incorporated-BC sample was rinsed with large amount of water. Finally, the obtained sample was dried by using the freeze drying technique. XRD patterns of the neat BC, the as-prepared magnetic particle incorporated-BC sample, the as-prepared silver particle incorporated-BC sample and the as-prepared magnetic and silver particle incorporated-BC sample were showed in the figure 5.6. The XRD pattern of neat BC exhibited the 2 characteristic peaks of BC at 2□ = 14.5° and 22.7°. These 2 characteristic peaks were corresponded to (110) and (220) planes, respectively which attributed to the typical profile of cellulose I allomorph (Retegi, Gabilondo, Peña, Zuluaga, Castro, Gañan, Caba, & Mondragon, 2010). This characteristic diffraction pattern was corresponded to the BC cultured in static culture (Yan, Chen, Wang, Wang, Wang, & Jiang, 2008). The XRD pattern of magnetic particle incorporated-BC exhibited the 6 characteristic diffraction peaks at 2□ = 30.40°, 35.81°, 43.53°, 54.02°, 57.59° and 63.25°. These characteristic diffraction peaks were corresponded to (220), (311), (400), (422), (511), and (440) planes, respectively (Guo *et al.*, 2009).

All these characteristic diffraction peaks indicated that the as-synthesized magnetic particles were in the form of magnetite (Fe_3O_4). Whereas, the XRD pattern of Ag particle incorporated-BC exhibited characteristic diffraction peaks at 2θ = 38.1°, 44.3°, 64.4° and 78.0°. These 4 characteristic diffraction peaks were corresponded to (111), (200), (220) and (311) planes, respectively (Zhang *et al.*, 2006).

The XRD pattern of magnetic and silver particle incorporated-BC exhibited all characteristic diffraction peaks of magnetic particle at 2□ = 30.40°, 35.81°, 43.53°, 54.02°, 57.59°, 63.25° and also silver particle at 2θ = 38.1°, 44.3°, 64.4°, 78.0°, respectively. According the XRD patterns, there were clearly revealed that the Magnetic and Ag particle were successfully incorporated into the matrix of BC. Moreover, the incorporated-magnetic particles were in the form of magnetite (Fe_3O_4) which exhibited the highest saturation magnetization in comparison with the others form of iron oxide (Katepetch, & Rujiravanit, 2011). The requirements for being as magneto-active material, the incorporated-magnetite (Fe_3O_4) particles with superparamagnetic property, were successfully achieved by using the ammonia gas-enhancing *in situ* co-precipitation method as evidences by VSM hysteresis loop and XRD patterns. Then, the requirements for being as electro-active material were investigated by using the TGA technique and the two points probe conductivity meter in order to examine the percent incorporation of silver particles and the electrical conductivity of the as-prepared magnetic and silver particle incorporated-BC sample, respectively.

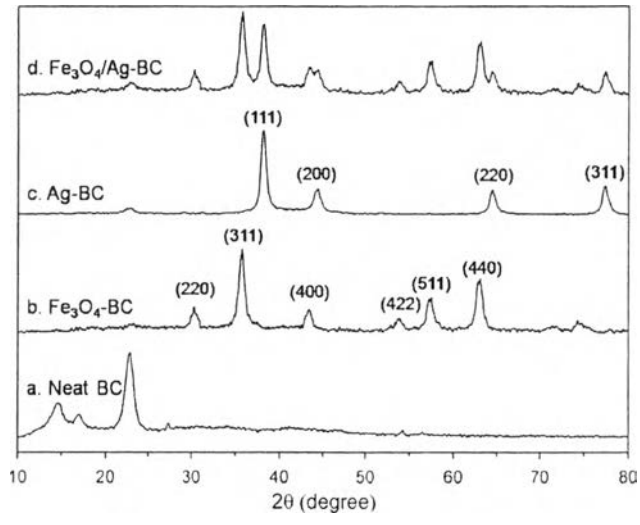

Figure 5.6 The XRD patterns of neat BC (a), magnetic particle incorporated-BC sample prepared by using 0.50 M of aqueous iron ion solution (b), silver particle incorporated-BC sample prepared by using 0.10 M of silver nitrate solution (c) and magnetic and silver particle incorporated-BC sample prepared by using 0.50 M of aqueous iron ion solution and followed by using 0.10 M of silver nitrate solution (d).

5.4.7 Thermal gravimetric analysis (TGA) of the magnetic and silver particle incorporated-BC sample

The TGA thermograms of the as-prepared magnetic and silver particle incorporated-BC sample were using for determining percent incorporation of the magnetic and silver particle in the as-prepared magnetic and silver particle incorporated-BC sample. The percent incorporation of silver particles in the as-prepared sample was determined by using method of Ghule *et al.*, (2006). TGA thermograms of the as-prepared magnetic and silver particle incorporated-BC sample show in the figure 5.7. Percent remaining residue of magnetic particle in the as-prepared magnetic particle incorporated-BC sample which prepared by using 0.50 M of aqueous iron ion solution were 70.17 ±0.26 wt%. Whereas, percent remaining residue of silver and magnetic particle in the as-prepared magnetic and silver particle incorporated-BC sample which prepared by using 0.01 M, 0.05 M and 0.10 M of silver nitrate were 72.50 ±2.24 wt%, 73.97 ±2.20 wt% and 81.35 ±1.82 wt%, respectively. Therefore, the percent incorporation of silver particles in the as-

prepared magnetic and silver particle incorporated-BC sample were determined by the difference in percent remaining residue when compared to the as-prepared magnetic particle incorporated-BC sample which prepared by using 0.50 M of aqueous iron ion solution. The percent incorporation of silver particles in the as-prepared magnetic and silver particle incorporated-BC sample prepared by using 0.50 M of aqueous iron ion solution and followed by using 0.01 M, 0.05 M and 0.10 M of silver nitrate solution were calculated to be 3.23 ±2.24 wt%, 4.70 ±2.20 wt% and 12.08 ±1.82 wt%, respectively.

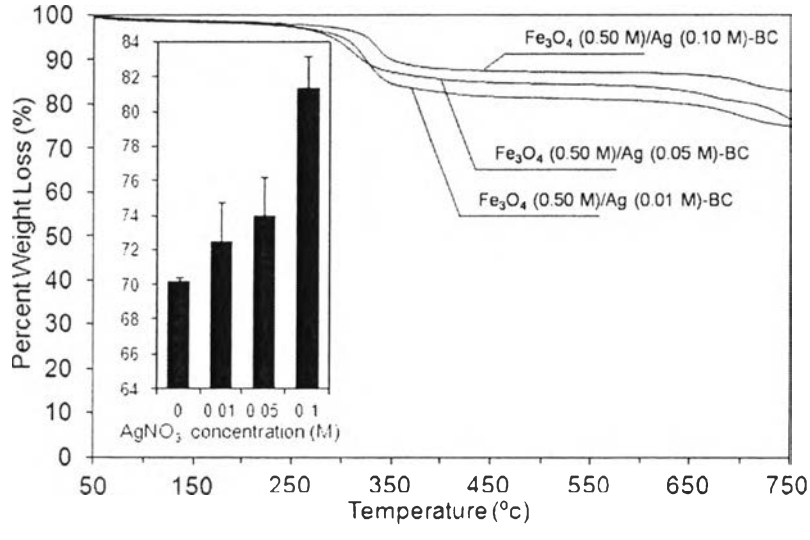

Figure 5.7 TGA thermograms of the magnetic and silver particle incorporated-BC samples prepared by sodium borohydride-enhancing *in situ* synthesis method with using 0.01 M, 0.05 M and 0.10 M of silver nitrate solution, respectively. Inset showed the percent remaining residue of magnetic and silver particle in the magnetic particle incorporated-BC in comparing with the as-prepared magnetic particle incorporated-BC sample.

5.4.8 The magnetic and electric properties of the as-prepared magnetic and silver particle incorporated-BC sample

Magnetic property of the as-prepared magnetic and silver particle incorporated-BC samples were examined by using VSM technique and representing in the form of magnetic hysteresis loop. Whereas, the electric property of as-prepared

magnetic and silver particle incorporated-BC samples were examined by using two points probe conductivity meter and representing in the form of electrical conductivity. The magnetic hysteresis loop of silver particle incorporated-BC sample, magnetic particle incorporated-BC sample and silver and magnetic particle incorporated-BC samples is showed in figure 5.8. The magnetic hysteresis loop of magnetic particle incorporated-BC sample was exhibited the saturation magnetization of 46.75 emu/g whereas the magnetic hysteresis loop of magnetic particle incorporated-BC sample was exhibited the saturation magnetization of 0.072 emu/g. The magnetic hysteresis loop of magnetic and silver particle incorporated-BC samples which prepared by using 0.50 M of aqueous iron ion solution and followed by using 0.01 M, 0.05 M and 0.10 M of silver nitrate solution were exhibited the saturation magnetization of 45.85emu/g, 39.9 emu/g and 25.53 emu/g, respectively. Saturation magnetization and coercive field of the silver particle incorporated-BC sample, the magnetic particle incorporated-BC sample and the magnetic and silver particle incorporated-BC sample were summarized in table 1. Saturation magnetization of the as-prepared magnetic and silver particle incorporated-BC samples were decreased with increasing of the concentration silver nitrate solution. These decreasing of the saturation magnetization of the as-prepared samples might resulted from the increasing of the weight of sample due to the increasing in percent incorporating of silver particles in the as-prepared samples. Coercive fields were considered as criteria for classified the superparamagnetic behavior of the as-prepared samples. Lower than 100 G in coercive fields, the as-prepared samples were classified as a superparamagnetic material. In order to function as a magneto-active material, the superparamagnetic behavior is the most important requirements. Coercive fields of the as-prepared magnetic and silver particle incorporated-BC samples prepared by using 0.50 M of aqueous iron ion solution and followed by using 0.01 M, 0.05 M and 0.10 M of silver nitrate solution were 32.62 G, 27.67 G and 25.18 G, respectively. The as-prepared samples were exhibited coercive fields with much lower than the critical criteria (100 G) therefore the as-prepared magnetic and silver particle incorporated-BC samples were exhibited the superparamagnetic behavior and classified as a magneto-active material.

Electrical property of the as-prepared magnetic and silver particle incorporated-BC samples were determined by using two points probe conductivity meter and presented in the term of electrical conductivity. Table 1 show electrical conductivity of the magnetic particle incorporated-BC sample and the magnetic and silver particle incorporated-BC samples the magnetic particle incorporated-BC sample. The magnetic particle incorporated-BC samples were exhibited the electrical conductivity of 0.0016 ±0.00028 S/cm whereas, the magnetic and silver particle incorporated-BC samples prepared by using 0.50 M of aqueous iron ion solution and followed by using 0.01 M, 0.05 M and 0.10 M of silver nitrate solution were exhibited the electrical conductivity of 0.0022 ±0.00012 S/cm, 1017.55 ±107.12 S/cm and 2009.55 ±105.75 S/cm, respectively. Regarding to electrical conductivity of the as-prepared samples, it was clearly revealed that the electrical property of the as-prepared samples was resulted from the incorporated-Ag particles. Electrical conductivity of the as-prepared were increased from 0.0022 ±0.00012 S/cm to 1017.55 ±107.12 S/cm and to 2009.55 ±105.75 S/cm with increasing of the concentration of silver nitrated solution from 0.01 M to 0.05 M and to 0.10 M, respectively. The increasing of electrical conductivity of the as-prepared sample might result from the increasing of the incorporated-silver particles (table1). The increasing in the amount of the incorporated-silver particles were increased the opportunity to form the connected bridge between particles. When the well connected-particles were achieved the overall electrical conductivity of the as-prepared materials were tremendous increased to over 10^3 S/cm and also changed the overall property of that material from semiconductor to conductor. The percent incorporation of silver particles which achieved the well connected-particles was called "the percolation threshold". In order to reach the percolation threshold, typically polymer based conductive formulations have very high silver loading (70-85 % by weight) (Bao, Wei, & Xiao, 2007). Anyways, the as-prepared magnetic and silver particle incorporated-BC samples were reached to the percolation threshold at the electrical conductivity of 1017.55 ±107.12 S/cm by incorporating only 4.70 ±2.20 wt% of silver. These might be resulted from the unique nanostructure of BC. Even incorporating of 62.31 wt% magnetic particles, the BC were still retained the unique structure of three-dimensional non woven network structure. This unique

structure was provided the continuous microporous for supporting the as-synthesizing silver particles. Therefore, the as-prepared magnetic and silver particle incorporated-BC samples were exhibited the electrical conductivity of 1017.55 ±107.12 S/cm at only 4.70 ±2.20 wt% of silver. According to these result, the requirement of effective electro-active material, to form the well connected of silver particles with optimizing the percent incorporation, was successfully achieved by using the sodium borohydride-enhancing *in situ* synthesis method. Moreover, the as-prepared magnetic and silver particle incorporated-BC samples were exhibited the very high electrical conductivity leading to also exhibit the very high electro-active properties.

These resulted were firmly supported the successfully preparing of the magnetic and silver particle incorporated-BC. Moreover, the as-prepared magnetic and silver particle incorporated-BC samples were also exhibited both properties of the incorporated-magnetic and silver particles. Hence, the magneto- and electro-active material was successfully prepared by incorporating of magnetic and silver particles into BC matrix.

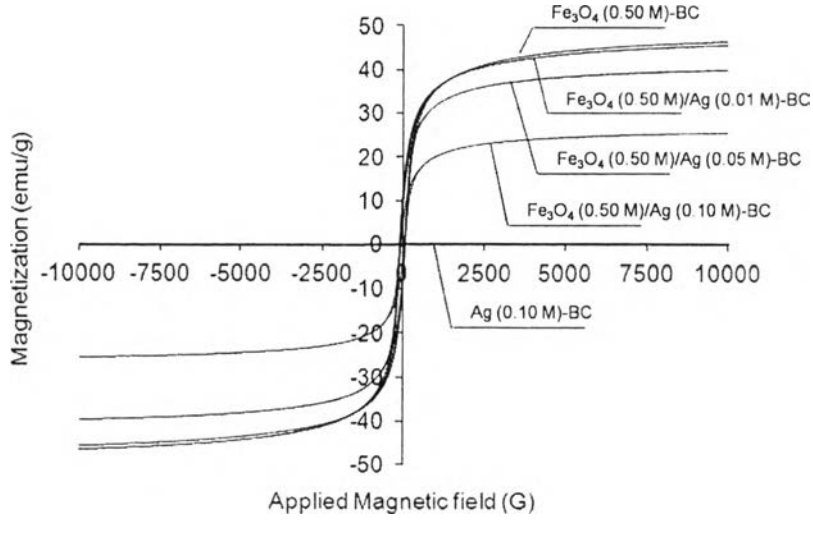

Figure 5.8 Magnetic hysteresis loop of silver particle incorporated-BC sample prepared by using 0.10 M of silver nitrate solution, magnetic particle incorporated-BC sample prepared by using 0.50 M of aqueous iron ion solution and magnetic and silver particle incorporated-BC sample prepared by using 0.50 M of aqueous iron ion

solution and followed by using 0.01 M, 0.05 M and 0.10 M of silver nitrate solution, respectively.

5.5 Conclusions

In this present study, the magneto- and electro-active material was successfully prepared by using step-wised incorporating process of magnetic and silver particles into BC matrix, respectively. Briefly, the magnetic particles were firstly incorporated into BC pellicle by immersing of BC pellicle into the aqueous iron ion solution then the iron ion absorbed-BC pellicle were treated with ammonia gas in the close system in order to prevent the side reaction with oxygen. By using the ammonia gas-enhancing *in situ* co-precipitation method, the incorporated-magnetic particles were presented in the form of magnetite particle (Fe_3O_4) with exhibited high saturation magnetization and very low coercive fields. The saturation magnetization of the as-prepared magnetic particle incorporated-BC sample were increased from 2.10 emu/g to 45.16 emu/g with increasing of the percent incorporation of magnetic particles from 20.37 ±0.10 wt% to 75.30 ±0.43 wt%, respectively. Moreover, the coercive fields of the as-prepared magnetic particle incorporated-BC sample were in the range of 33.14-34.30 G which could be able to classify the as-prepared samples as a superparamagnetic material. Moreover, the unique three -dimensional nonwoven structure of BC still existed even at 62.31 ±0.68 wt% of magnetic particles. For incorporating of the silver particles, the obtained magnetic particle incorporated-BC pellicles were used as a template. The magnetic particle incorporated-BC pellicles were immersed in silver nitrate solution. Then, the silver ion-absorbed magnetic particle incorporated-BC pellicles were immersed in sodium borohydride solution. While immersing in the sodium borohydride solution, the absorbed-silver ions were reduced to silver particles and precipitated inside the matrix of magnetic particle incorporated-BC pellicle. The as-prepared magnetic and silver particle incorporated-BC samples were exhibited both unique properties of magnetic and silver particles. The as-prepared magnetic and silver particle incorporated-BC samples were exhibited the saturation magnetization in the range of 25.53- 45.85emu/g with the coercive field of 25.18-32.62 G whereas

the prepared magnetic and silver particle incorporated-BC samples were also exhibited the electrical conductivity in the range of 0.0022 ±0.00012-2009.55 ±105.75 S/cm with the 3.23 ±2.24-12.08 ±1.82 wt% of the incorporated-silver particles. The as-prepared magnetic and silver particle incorporated-BC samples were exhibited the percolation threshold at 4.70 ±2.20 wt% of silver particle with the electrical conductivity of 1017.55 ±107.12 S/cm. These evidences were firmly supported the successfully preparing of the magnetic and silver particle incorporated-BC and the unique properties of the two incorporated-particles were still existed therefore the as-prepared magnetic and silver particle incorporated-BC were exhibited the magneto- and electro-active properties of the incorporating particles. Moreover, this new proposed-preparation method was surprisingly simple and cost-effective, which may provide a facile approach toward the manufacturing of metal oxide nanocomposites, low-temperature catalysts, electromagnetic shielding and other useful materials. By using this preparation method, the magnetically and electrically responsive properties also could be achieved into the other materials such as electro-spun nanofiber mat and other porous materials.

le 5.1 Magnetic and electric properties of magnetic particle incorporated-BC sample prepared by using 0.50 M of aqueo
tion (a) and magnetic and silver particle incorporated-BC samples prepared by using 0.50 M of aqueous iron ion so
wed by using 0.01 M (b), 0.05 M (c) and 0.10 M (d) of silver nitrate solution, respectively

Sample References	Percent Incorporation (wt%)		Magnetization (emu/g)	Coercive field (E)	Condu (S/c
	Magnetic	Silver			
e_3O_4/Ag (0.01 M)-BC	62.31 ±0.68	3.23 ±2.24	45.85	32.62	0.0022 ±
e_3O_4/Ag (0.05 M)-BC	62.31 ±0.68	4.70 ±2.20	39.90	27.67	1017.55
e_3O_4/Ag (0.10 M)-BC	62.31 ±0.68	12.08 ±1.82	25.53	25.18	2009.55
e_3O_4/(0.50 M)-BC	62.31 ±0.68	-	46.75	34.16	0.0016 ±

5.6 Acknowledgements

This work is greatly supported in cash and in kind by the Chulalongkorn University Dutsadi Phiphat Scholarship, the Rachadapisek Somphot Endowment Fund, The Petroleum and Petrochemical College, Chulalongkorn University, Center of Excellence on Petrochemical and Materials Technology, The Conductive and Electroactive Polymers Research Unit and Kansai University, Japan, are greatly acknowledged.

5.7 References

Bao, L., Wei, B., & Xiao, A. Y. (2007). Conductive Coating Formulations with Low Silver Content, *IEEE 57th electronic components and technology conference, 2*, 494–500.

Cornell, R. M., & Schwertmann, U. (2003). The iron oxides: structure, properties, reactions, occurrences and uses (2nd ed.). Weinheim: Wiley-VCH.

Czaja, W. K., Romanovicz, D., & Brown, R. M. (2004). Structural investigations of microbial cellulose produced in stationary and agitated culture. *Cellulose, 11*, 403–411.

Czaja, W. K., Young, D. J., Kawecki, M., & Brown, R. M. (2007). The future prospects of microbial cellulose in biomedical applications. *Biomacromolecules, 8*, 1–12.

Davis, L. C. (1999). Model of magnetorheological elastomers, *Journal of Applied Physics, 85(6)*, 3348–3351.

Dikeakos, M., Tung, L. D., Veres, T., Stancu, A., Spinu, L., & Normandin, F. (2003). Fabrication and characterization of tunable magnetic nanocomposite materials. Materials Research Society Symposium Proceedings, 734, 315–320.

Dubey, V., Saxena, C., Singh, L., Ramana, K. V., & Chauhan R. S. (2002) Pervaporation of binary water–ethanol mixtures through bacterial cellulose membrane. *Separation and Purification Technology, 27*, 163–171.

Epstein, A. J., & Miller, J. S. (1996). Molecule- and polymer-based magnets, a new frontier. Synthetic Metals, 80, 231–237.

Filipcsei, G., Csetneki, I., Szilágyi, A., & Zrínyi, M. (2007). Magnetic field-responsive smart polymer composites. Advances in Polymer Science, 206, 137–189.

Fugetsua, B., Sanob, E., Sunadac, M., Sambongic, Y., Shibuyac, T., Wangd, X., & Hirakid, T. (2008). Electrical conductivity and electromagnetic interference shielding efficiency of carbon nanotube/cellulose composite paper. *carbon, 46*, 1253–1269.

Ghule, K., Ghule, A. V., Chen B., & Ling, Y. (2006). Preparation and characterization of ZnO nanoparticles coated paper and its antibacterial activity study. *Green Chemistry, 8*, 1034–1041.

Grzegorczyn, S., & Ezak, A. (2007). Kinetics of concentration boundary layers buildup in the system consisted of microbial cellulose biomembrane and electrolyte solutions. *Journal of Membrane Science, 304*, 148–155.

Guo, J., Ye, X., Liu, W., Wu, Q., Shen, H., & Shu, k. (2009). Preparation and characterization of poly(acrylonitrile-co-acrylic acid) nanofibrous composites with Fe_3O_4 magnetic nanoparticles. *Materials Letters, 63*, 1326–1328.

Hiamtup, P., Sirivat, A., & Jamieson, A. M. (2008). Electromechanical response of a soft and flexible actuator based on polyaniline particles embedded in a cross-linked poly(dimethyl siloxane) network. Materials *Science and Engineering C, 28*, 1044–1051.

Hu, W., Chen, S., Li, X., Shi, S., Shen, W., Zhang, X., & Wang, H. (2009). *In situ* synthesis of silver chloride nanoparticles into bacterial cellulose membranes. *Materials Science and Engineering C, 29*, 1216–1219.

Jiles, D. (1991). Introduction to magnetism and magnetic materials. London: Chapman & Hall/CRC.

Kamel, S. (2007). Nanotechnology and its applications in lignocellulosic composites, a mini review. *eXPRESS Polymer Letters, 1*, 546–575.

Katepetch, C., & Rujiravanit, R. (2011). Synthesis of magnetic nanoparticle into bacterial cellulose matrix by ammonia gas-enhancing in situ co-precipitation method. *Carbohydrate Polymers, 86*, 162–170.

Klemm, D., Schumann, D., Udhardt, U., & Marsch, S. (2001). Bacterial synthesized cellulose-artificial blood vessels for microsurgery. *Progress in Polymer Science, 26(9)*, 1561–1603.

Li, X., Chen, S., Hu, W., Shi, S., Shen, W., Zhang, X. & Wang H. (2009). In situ synthesis of CdS nanoparticles on bacterial cellulose nanofibers. *Carbohydrate Polymers, 76*, 509–512.

Ludeelerd, P., Niamlang, S., Kunaruksapong, R., & Sirivat, A. (2010). Effect of elastomer matrix type on electromechanical response of conductive polypyrrole/elastomer blends. *Journal of Physics and Chemistry of Solids, 71*, 1243–1250.

Majewski, P., & Thierry, B. (2007). Functionalized magnetite nanoparticles—Synthesis, properties, and bio-applications. Critical Reviews in Solid State and Materials Science, 32, 203–215.

Maneerung, T., Tokura, S., & Rujiravanit, R. (2008). Impregnation of silver nanoparticles into bacterial cellulose for antimicrobial wound dressing. *Carbohydrate Polymers, 72*, 43–51.

Neuberger, T., Schopf, B., Hofmann, H., Hofmann, M., & Rechenberg, B. (2005).Superparamagnetic nanoparticles for biomedical applications: Possibilities and limitations of a new drug delivery system. *Journal of Magnetism and Magnetic Materials, 293*, 483–496.

Niamlang, S., & Sirivat, A. (2009). Electrically controlled release of salicylic acid from poly(p-phenylene vinylene)/polyacrylamide hydrogels. *International Journal of Pharmaceutics, 371*, 126–133.

Paquette, J.W., Kim, K. J., & Kim, D. (2005). Low temperature characteristics of ionic polymer–metal composite actuators. *Sensors and Actuators A, 118*, 135–143.

Retegi, A., Gabilondo, N., Peña, C., Zuluaga, R., Castro, C., Gañan, P., Caba, K., & Mondragon, I. (2010). Bacterial cellulose films with controlled microstructure–mechanical property relationships. *Cellulose, 17*, 661–669.

Rezaee, A., Solimani, S., & Forozandemogadam, M. (2005). Role ofplasmid in production of Acetobacter xylinum biofilms. *American Journal of Biochemistry and Biotechnology, 1*, 121–125.

Roman, M., & Winter, W. T. (2004). Effect of sulfate groups from sulfuric acid hydrolysis on the thermal degradation behavior of bacterial cellulose. *Biomacromolecules, 5*, 1671–1677.

Stauffer, D. & Aharony, A., (1992). Introduction to Percolation Theory. Taylor & Francis, 1992, Chapter 1.

Tartaj, P., Morales, M. D., Veintemillas-Verdaguer, S., Gonzalez-Carreno, T., & Serna, C. J. (2003). The preparation of magnetic nanoparticles for applications in biomedicine. Journal of Physics D: Applied Physics, 36, R182–R197.

Thuwachaowsoan, K., Chotpattananont, D., Sirivat, A., Rujiravanit, R., & Schwank J. W. (2007) Electrical conductivity responses and interactions of poly(3-thiopheneacetic acid)/zeolites L, mordenite, beta and H2. *Materials Science and Engineering B, 140*, 23–30.

Wang, M., Singh, H., Hatton, T. A., & Rutledge, G. C. (2004). Field-responsive superparamagnetic composite nanofibers by electrospinning. *Polymer, 45*, 5505–5514.

Wan, Y., Hong, L., Jia, S., Huang, Y., Zhu, Y., Wang, Y., & Jiang, H. (2006). Synthesis and characterization of hydroxyapatite-bacterial cellulose nanocomposites. *Composites Science and Technology, 66*, 1825–1832.

Yan, Z., Chen, S., Wang, H., Wang, B., Wang, C., & Jiang, J. (2008). Cellulose synthesized by Acetobacter xylinum in the presence of multi-walled carbon nanotubes. *Carbohydrate Research, 343*, 73–80.

Zhang, D., & Qi, L. (2005). Synthesis of mesoporous titania networks consisting of anatase nanowires by templating of bacterial cellulose membranes. *Chemical Communications, 21*, 2735–2737.

Zhang, J., Liu, K., Dai, Z., Feng, Y., Bao, J., & Mo, X. (2006). Formation of novel assembled silver nanostructures from polyglycol solution. *Materials Chemistry and Physics, 100*, 106–112.